ResearchGate

See discussions, stats, and author profiles for this publication at: https://www.researchgate.net/publication/263774445

Assessing soil constituents and labile soil organic carbon by mid-infrared photoacoustic spectroscopy

Article *in* Soil Biology and Biochemistry · October 2014

DOI: 10.1016/j.soilbio.2014.06.022

CITATIONS
16

READS
303

5 authors, including:

Clément Peltre
University of Copenhagen
30 PUBLICATIONS **177** CITATIONS
SEE PROFILE

Sander Bruun
University of Copenhagen
104 PUBLICATIONS **1,275** CITATIONS
SEE PROFILE

Chang-Wen Du
Chinese Academy of Sciences
103 PUBLICATIONS **818** CITATIONS
SEE PROFILE

Lars Stoumann Jensen
University of Copenhagen
144 PUBLICATIONS **4,531** CITATIONS
SEE PROFILE

Some of the authors of this publication are also working on these related projects:

Optimisation of value chains for biogas production in Denmark (Biochain) View project

All content following this page was uploaded by Clément Peltre on 09 July 2014.

The user has requested enhancement of the downloaded file. All in-text references underlined in blue are added to the original document and are linked to publications on ResearchGate, letting you access and read them immediately.

Soil Biology & Biochemistry 77 (2014) 41–50

Contents lists available at ScienceDirect

Soil Biology & Biochemistry

journal homepage: www.elsevier.com/locate/soilbio

Assessing soil constituents and labile soil organic carbon by mid-infrared photoacoustic spectroscopy

Clément Peltre [a, *], Sander Bruun [a], Changwen Du [b], Ingrid K. Thomsen [c], Lars S. Jensen [a]

[a] Department of Plant and Environmental Sciences, Faculty of Science, University of Copenhagen, Thorvaldsensvej 40, Frederiksberg C DK-1871, Denmark
[b] State Key Laboratory of Soil and Sustainable Agriculture, Institute of Soil Science, Chinese Academy of Sciences, Nanjing 210008, China
[c] Department of Agroecology, Aarhus University, PO Box 50, Tjele DK-8830, Denmark

ARTICLE INFO

Article history:
Received 25 March 2014
Received in revised form
23 June 2014
Accepted 28 June 2014
Available online 3 July 2014

Keywords:
FTIR-PAS
NIR
Soil carbon
Soil organic matter
Stability

ABSTRACT

Recent progress in microphone sensitivity has dramatically increased the performance of Fourier transform mid-infrared photoacoustic spectroscopy (FTIR-PAS). This technique offers benefits over reflectance spectroscopy techniques because the level of sample reflectance has little effect on the PAS signal. This also means that it should be advantageous for soil analysis because of its highly opaque nature. However, only a limited number of studies have so far applied FTIR-PAS to soil characterization and investigation is still required into its potential to determine soil organic carbon (SOC) degradability. The objective of this study was to assess the potential of FTIR-PAS for the characterisation of the labile fraction of SOC and more classical soil parameters, such as carbon and clay content, for a range of 36 soils collected from various field experiments in Denmark. Partial least squares (PLS) regression was used to correlate the collected FTIR-PAS spectra with the proportion of soil organic carbon mineralised after 238 days of incubation at 15 °C and pF 2 (C_{238d}) taken as an indicator of the labile fraction of SOC. Results showed that it is possible to predict total organic carbon content, total nitrogen content and the labile fraction of SOC using FTIR-PAS with an accuracy similar to or better than near infrared (NIR) spectroscopy. FTIR-PAS offered the advantage over NIR of allowing identification of chemical compounds that correlated positively or negatively with the labile fraction of SOC. Spectral bands corresponding to aliphatic, methyl, amide III and polysaccharides compounds were positively correlated with C_{238d}, whereas bands corresponding to aromatics, amines, amides II and carboxylic acids were negatively correlated with C_{238d}. In conclusion, FTIR-PAS has proved to be a powerful tool for characterising soil composition and its labile SOC fraction, offering several benefits over reflectance spectroscopy techniques.

© 2014 Elsevier Ltd. All rights reserved.

1. Introduction

The persistence of soil organic matter is recognised as a major ecosystem property due to its key role in earth carbon cycling, soil quality and ecosystem services (Schmidt et al., 2011). Soil organic carbon (SOC) stability is defined in terms of its resistance to microbial decomposition. It is typically studied using biological methods such as the measurement of CO_2–C evolution during laboratory incubations, allowing a labile fraction of SOC decomposed during the incubation period to be separated from a stable fraction (Paul et al., 2006; Thomsen et al., 2009). However these methods are time consuming and there is still a need for reliable techniques to be developed to characterise SOC stability, providing both quantitative measurements and qualitative information, in order to improve understanding of the mechanisms controlling SOC persistence.

Several spectroscopic methods have been used to characterise and predict soil constituents and SOC stability. Near infrared reflectance (NIR) spectroscopy has provided accurate predictions of the mineralisation of SOC (Chang et al., 2001; Thomsen et al., 2009), exogenous organic matter (Peltre et al., 2011) and plant residues (Bruun et al., 2005). However, one major drawback of NIR is that it does not allow in-depth interpretation of the molecular vibrations associated with spectral regions correlated with SOC stability. This is due to the fact that absorption in the near infrared range (800–2500 nm) originates from overtones and combination bands of fundamental molecular vibrations where there is considerable overlap (Wetzel, 1983). Mid-infrared spectroscopy (in the range of 4000–400 cm^{-1}) allows the correct identification of spectral regions corresponding to vibrations of specific functional groups. Transmittance spectroscopy is the oldest mid-infrared method. For

* Corresponding author.
E-mail addresses: peltre@plen.ku.dk, cpeltre@yahoo.fr (C. Peltre).

http://dx.doi.org/10.1016/j.soilbio.2014.06.022
0038-0717/© 2014 Elsevier Ltd. All rights reserved.

soil analysis, the method requires the preparation of pellets made of finely ground soil mixed with KBr powder. Mid-infrared transmittance spectroscopy has traditionally been used for molecular characterisation of SOM (Stevenson, 1994; Gerzabek et al., 2006). The use of mid-infrared spectroscopy has subsequently been generalised to the prediction of diverse soil characteristics by the development of mid-infrared reflectance (MIR) spectroscopy and the improvement of computing power, allowing the calculation of advanced chemometric methods such as partial least squares (PLS) regression. Diffuse reflectance infrared Fourier transform (DRIFT) spectroscopy and attenuated total reflectance Fourier transform infrared (FTIR-ATR) spectroscopy allow the analysis of soil samples without preparation of KBr pellets, which dramatically increases the speed of analysis. Reflectance mid-infrared spectroscopy has been shown to perform as well, if not better than NIR spectroscopy for the prediction of diverse soil properties (Viscarra Rossel et al., 2006; Soriano-Disla et al., 2013), and allows interpretation of the spectral ranges used for predictions (Leifeld, 2006; Janik et al., 2007; Cecillon et al., 2012). However, reflectance spectroscopy for soil analysis raises some difficulties related firstly to the low reflectance of some soils, and secondly to the high influence of particle size and grinding (Stumpe et al., 2011). Therefore, soil dilution with KBr powder has often been used to avoid spectral distortion and nonlinearities in DRIFT spectra (e.g. Nguyen et al., 1991; Capriel et al., 1995; van Groenigen et al., 2003). The FTIR-ATR technique is also not optimal because of the poor optical contact between soil particles and the ATR diamond probe and because the limited area scanned generally makes it difficult to integrate sample variability.

In the last three decades, progress in microphone sensitivity has dramatically increased the performance of Fourier transform mid-infrared photoacoustic spectroscopy (FTIR-PAS). This technique is based on the absorption of an infrared beam by the sample, creating absorption-induced heating, which in turn produces thermal expansion-driven pressurisation in the surrounding gas, known as the PAS signal. This is detected by a microphone and computer-transformed into a spectrum (McClelland et al., 2006). FTIR-PAS is particularly suited to dark samples, such as soil, organic waste, manure or biochar, which typically have low reflectance. Despite the high potential of FTIR-PAS for soil analysis, only a very limited number of studies have applied FTIR-PAS for SOM characterisation, and its potential for determining SOC degradability still requires investigation (Churchman et al., 2010; Du and Zhou, 2011; Pedersen et al., 2011; Du et al., 2013).

The objective of this study was to assess the potential of FTIR-PAS for the characterisation of the labile fraction of SOC determined during aerobic laboratory incubation and more classical soil parameters, such as total organic carbon, total nitrogen and clay content, for 36 soils collected from various fields in Denmark (Thomsen et al., 2009). The hypothesis was that FTIR-PAS can predict SOC degradability with similar or greater accuracy compared to NIR, while allowing in-depth interpretation of chemical compounds that correlate positively or negatively with the various soil constituents.

2. Materials and methods

The results of the incubation experiment in Thomsen et al. (2009) were reused for the current study. For convenience the soil samples and incubation procedure is described briefly below.

2.1. Soil samples

Three sets of soils were collected from 0 to 20 cm horizons of arable fields across Denmark, in total 36 different soil samples (Table 1). The first set of soils was retrieved in 2002 during experimental treatments with varying organic matter (OM) inputs with straw removal, straw incorporation or straw burning in Jyndevad, Askov and Rønhave and during experimental treatments involving unfertilised, mineral fertiliser (NPK) and animal manure amendment in the Askov long-term experiment. A second set included soils sampled within fields with in-situ gradients in soil texture or OM content. The Vildbjerg, Aulum and Lerbjerg sites feature gradients of clay content, and the Sørvard site feature a gradient of OM content. The third set of soils included soil retrieved from single field samplings. A more detailed description of the soil sample set can be found in Thomsen et al. (2009). The soils were air dried and sieved <2 mm prior to further analysis.

2.2. Labile fraction of SOC determined during incubation experiment

The soils were packed into a 100 cm^{-3} stainless steel cylinder by sequentially filling four portions of soil into the cylinder. Each individual portion was compressed with a manual tamper before the next portion was added. Soil water potential was adjusted to a matric potential of −100 hPa (pF 2). The excess soil due to soil swelling from adding water was trimmed to maintain a constant volume of 100 cm^{-3}. The final bulk density of the soil cores can be found in Table 1 (Thomsen et al., 2009). The cylinders were then placed in 2 L hermetically sealed jars with three replicates and incubated at 20 °C for 238 days (34 weeks). The evolved CO_2 was trapped in 20 mL of 0.5 M NaOH which was periodically replaced and titrated at days 3, 7, 14, 21, 28, 35, 42, 56, 70, 84, 105, 126, 147, 168, 189, 211 and 238. The water content of the soil was adjusted on day 21 and subsequently after every second replacement of NaOH. The cumulative amount of CO_2–C evolved after 238 days was expressed as a percentage of the initial SOC (C_{238d}, Table 1) and used as an indicator of the fraction of labile SOC.

2.3. Fourier transform mid-infrared photoacoustic spectroscopy (FTIR-PAS) and near infrared (NIR) spectroscopy

FTIR-PAS spectra were recorded on archived air-dried and <2 mm-sieved soils using a Bruker Tensor 27 spectrometer (Bruker corp. Billerica, MA, USA) equipped with a PA301 photoacoustic detector with a cantilever microphone (Gasera Ltd., Turku, Finland). Spectra were recorded as an average of 32 scans within the spectral range 4000–600 cm^{-1} in 2 cm^{-1} intervals. The soils were packed in 10 mm ring cups and inserted in the PAS detector with helium as the purge gas to increase detector sensitivity.

The near infrared spectra were retrieved from a previous study (Thomsen et al., 2009). Briefly, NIR spectra were recorded on a NIRSystem 6500 spectrometer (Foss Tecator) in the range 400–2500 nm in 2 nm intervals. For this study, the visible part of the spectra (400–799 nm) was removed because preliminary analyses revealed better performance with only the NIR range (800–2500 nm). The air-dried and 2 mm-sieved soils were packed in 36 mm spinning ring cups and spectra were recorded as the average of 16 scans. The spectra were converted from reflectance (R) to absorbance (A) unit by $A = \log(1/R)$.

2.4. Statistical analyses

A principal component analysis (PCA) of the FTIR-PAS spectra was performed using R 2.15.3 with the ade4 package (Chessel et al., 2004; R Development Core Team, 2012). Spectra were smoothed using the Savitzky–Golay algorithm on three data points on both sides, and normalised by the sum of the absorbance on the whole spectra prior to PCA analysis.

Table 1
Soil designation, including field experiments and experimental treatment. Selected soil characteristics: texture, pH, organic C, total N (in mg g^{-1}), C:N, Bulk density and fraction of TOC evolved as CO_2 after 238 days of laboratory incubation, taken as an indicator of the labile fraction of soil organic C (C_{238d}).

	Soil designation	Clay (<2 μm)	Silt (2–63 μm)	Sand (63–2000 μm)	pH	TOC	Total N	C:N	Bulk density	C_{238d}
		(g kg^{-1})				(g kg^{-1})			(Mg m^{-3})	(% of initial TOC)
Samplings within experimental treatments										
Jyndevad (Humic Podzol)										
Straw removed	Jyn_SR	61	43	867	6.4	16.3	1.1	14.8	1.480	2.39
Straw incorporated	Jyn_SI	56	53	862	6.8	16.9	1.2	14.1	1.442	2.64
Straw burned	Jyn_SB	60	44	871	6.7	14.8	1.0	14.8	1.464	3.11
Askov (Stagnic Albeluvisol)										
Straw removed	Ask_SR	109	200	673	6.7	10.6	1.0	10.6	1.481	4.85
Straw incorporated	Ask_SI	105	202	671	6.6	13.1	1.2	10.9	1.456	6.29
Straw burned	Ask_SB	105	228	648	6.7	11.1	1.0	11.1	1.455	4.24
Rønhave (Orthic Luvisol)										
Straw removed	Røn_SR	143	337	503	6.5	10.1	1.2	8.4	1.435	4.36
Straw incorporated	Røn_SI	133	330	520	6.6	10.1	1.2	8.4	1.438	4.97
Straw burned	Røn_SB	142	329	509	6.8	11.6	1.4	8.3	1.404	6.10
Askov LTE										
Unfertilised	LTE_0	120	264	595	6.5	12.6	0.9	14.0	1.405	4.40
1 NPK	LTE_NPK	126	249	605	6.5	11.5	1.0	11.5	1.356	5.74
1.5 N in animal manure	LTE_AM	110	240	623	6.8	15.9	1.3	12.2	1.344	3.81
Sampling within a field with a textural or OM gradient										
Vildjerg (Haplic Podzol to Stagnic Luvisol)	Vild_CL1	73	122	782	6.6	13.7	1.2	11.4	1.415	3.39
	Vild_CL2	129	114	728	6.6	17.1	1.5	11.4	1.354	2.78
	Vild_CL3	185	130	650	7.0	20.7	1.8	11.5	1.294	3.02
	Vild_CL4	237	200	528	7.0	20.8	1.7	12.2	1.314	4.00
Sørvard (Haplic Podzol)	Sør_OM1	62	83	841	5.2	8.4	0.9	9.3	1.526	8.84
	Sør_OM2	57	73	841	5.7	17.0	1.3	13.1	1.373	4.69
	Sør_OM3	51	59	860	5.2	17.7	1.4	12.6	1.386	3.47
	Sør_OM4	46	68	842	6.0	26.4	2.0	13.2	1.294	4.21
Aulum (Haplic Podzol)	Au_CL1	46	51	892	6.0	6.6	0.6	11.0	1.552	7.81
	Au_CL2	51	60	878	6.4	6.5	0.6	10.8	1.531	9.28
	Au_CL3	94	231	654	5.9	12.3	1.0	12.3	1.375	6.69
Lerbjerg (Stagnic Luvisol to Stagnic Stagnosol)	Ler_CL1	109	116	749	6.7	15.2	1.5	10.1	1.303	5.25
	Ler_CL2	166	155	652	6.7	15.8	1.7	9.3	1.241	7.28
	Ler_CL3	251	143	578	6.8	16.5	1.9	8.7	1.184	8.30
	Ler_CL4	303	166	504	7.5	15.6	1.6	9.8	1.126	9.62
	Ler_CL5	402	144	392	7.6	16.1	1.7	9.5	1.051	12.33
Single field sampling										
Kvong (Arenic Umbrisol)	Kvo	79	272	617	6.4	18.6	1.7	10.9	1.348	4.47
Lybæk (Arenic Umbrisol)	Lyb	41	52	879	6.6	16.7	1.2	13.9	1.470	4.34
Kølkær (Densic Podzol)	Køl	46	48	861	6.6	26.1	1.4	18.6	1.392	2.51
Tvis (Densic Podzol)	Tvi	36	75	865	6.5	14.2	1.0	14.2	1.504	3.12
Fole (Stagnic Podzol)	Fol	124	192	658	6.8	15.1	1.6	9.4	1.341	6.33
Bjerndrup (Gleyic Podzol)	Bje	89	195	684	6.8	18.5	1.6	11.6	1.405	4.18
Dronninglund (Humic Dystric Cambisol)	Dro	89	325	500	6.3	50.7	2.5	20.3	1.127	1.72
Nakskov (Gleyic Luvisol)	Nak	186	303	474	6.9	15.6	1.7	9.1	1.328	5.64

Partial least squares (PLS) regressions were carried out using The Unscrambler software V. 10.3 (Camo Software, Oslo, Norway). Because we aimed at keeping sample preparation to its minimum, and at avoiding any alteration of soil organic matter, no additional drying was performed prior to FTIR-PAS analysis. The residual soil moisture might affect the absorption in the region 4000–3000 cm^{-1}. This region was therefore excluded from the PLS regression analysis in order to avoid adverse effects from residual soil moisture. Preliminary analyses showed better PLS model performance with just the 3000–600 cm^{-1} range, which agrees with the findings of Leifeld (2006) who concluded that this band was not contributing to the quantification of organic compounds. Mathematical pre-treatment of the FTIR-PAS spectra prior to PLS regression analysis included smoothing using the Savitzky–Golay algorithm on three data points on both sides, as well as baseline offset and normalisation by the area under spectra. The NIR spectra were mathematically pre-treated by applying the Savitzky–Golay second derivative and smoothing four data points on both sides, as suggested by Thomsen et al. (2009). For combined FTIR-PAS and NIR model calibration, the previously mathematically pre-treated FTIR-PAS and NIR data were juxtaposed in a single data table and used as X-variables for PLS regression. Leave-3-out cross-validation was computed on in order to determine the optimal number of factors to retain in the PLS models and calculate validated predictions. The goodness of fit was assessed using the coefficient of determination R^2, root mean square error of cross validation on calibration (R^2 and RMSE) and cross-validated predictions (R^2CV and RMSECV). The ratio of performance to deviation (RPD) was calculated as the ratio of standard deviation of measured data to RMSECV. For soil analyses, a PLS model with an RPD ratio >2.5 can be considered as good for prediction purposes, while an RPD between 2 and 2.5 can be considered as approximate and RPD <2 as insufficient for prediction (Chang et al., 2001). The soil from the Dronninglund site was removed from the PLS analysis for TOC and total N prediction because it showed much higher TOC and total N concentrations compared to the rest of the samples (50.7 g kg^{-1} for TOC and 2.5 g kg^{-1} for total N, Table 1).

3. Results

3.1. Soil characteristics

The total organic carbon (TOC) content of the soils ranged from 6.5 to 50.7 g kg^{-1} (average 16.0 g kg^{-1}), reflecting the different

arable use of the soils (Table 1). The total N content of the soils ranged from 0.6 to 2.5 g kg^{-1}, the C:N ratio from 8.3 to 20.3 and the clay content from 36 to 402 g kg^{-1}. While most of the soils had a sandy texture, the soils from the clay gradients at Vildjerg and Lerbjerg displayed much higher clay contents, reaching a maximum of 402 g kg^{-1} for the Ler_CL5 soil. The soils' pH ranged from 5.2 to 7.6 (average 6.5), which is typical for arable soils in Denmark. The fraction of TOC evolved as CO_2 after 238 days of incubation (C_{238d}) ranged from 1.72 to 12.33%, with 5.17% on average.

3.2. FTIR-PAS spectra

The spectra of the 36 soils generally featured common peaks, but with different intensities (Fig. 1). The interpretation of the major peaks, based on literature (Table 2) is detailed below. It should be noted that some functional groups or molecule vibrations relevant for interpreting SOC quality might not be visible because they are only present as a shoulder or overlapping with other bond vibrations. The application of chemometric statistics is necessary to identify these regions and this is detailed in the sections below. The spectra featured a peak at 3620 cm^{-1} attributed to the stretching vibration (ν) of O–H in clay minerals; a broad band spanning 3500–3000 cm^{-1} attributed to ν_{O-H} from water, alcohols, carboxylic acids, phenols and ν_{N-H} from amides; twin peaks at 2920 and 2850 cm^{-1} superimposed with the broad ν_{O-H} band typically attributed to ν_{C-H} of aliphatic methyl and methylene; three peaks centred at 1990, 1875 and 1785 cm^{-1} corresponding to quartz overtones; a broad peak centred at 1620 cm^{-1} spanning approximately the range 1740–1600 cm^{-1} gathering the overlapping vibration of $\nu_{C=O}$ from carboxylic acids at 1720–1710 cm^{-1} and amides at 1660–1650 cm^{-1}; $\nu_{C=C}$ from aromatics between 1660 and 1600 cm^{-1} conjugated with ν_{H-O-H} from associated water at 1630 cm^{-1} and δ_{N-H} from amine at 1610 cm^{-1}; a shoulder at 1540 cm^{-1} attributed to ν_{COO-}, ν_{N-H} and ν_{C-N} from carboxylates and amides and a peak at 1430 cm^{-1} corresponding to carbonates superimposed on a methyls ν_{C-H} band at 1445–1350 cm^{-1}. The shoulder at 1235 cm^{-1} can be assigned to C–H in-plane vibration from aromatic groups, whereas the large band spanning 1200–900 groups together the vibrations of ν_{C-O} from polysaccharides at 1170–1060 cm^{-1}, ν_{Si-O} from quartz at 1100–1000 cm^{-1} as well as δ_{C-O} from carbohydrates at 1050 cm^{-1} and ν_{Si-O} from clay minerals at 1030–950 cm^{-1}, δ_{C-H} from aromatics and δ_{Al-OH} from kaolinite and smectite at 975–800 cm^{-1}. It is therefore a region with a large number of overlaps. The region <800 cm^{-1} is dominated by the

Table 2
Absorption bands in the mid-infrared range and functional groups or soil components. Assignment based on literature studies. ν denotes stretching vibration and δ bending vibration.

Wavenumber (cm^{-1})	Vibration	Functional group or component
3620	νO–H	Clay minerals[a–e]
3600–2800	νO–H, νN–H	Water, alcohols and phenols; carboxyl and hydroxyl groups, amides[f-t]
3000–2800	νC–H	Aliphatic methyl and methylene groups[f-t]
2520	CO_3^{2-}	Carbonates[f,k,o]
2200–2000	Overtone νCOH	Carbohydrates[n]
2000–1790		Quartz overtones[c]
1720–1710	νC=O	Carboxylic acids[f,j,l,n]
1660–1640	νC=O	Amides[d,l,n,o]
1660–1600	νC=C	Aromatics[i,j,m,o]
1630	νH–O–H	Clay-bound water[d,f]
1610	δN–H	Amine[d]
1600–1570	νC=C, νCOO^-	Aromatics[f,i,o], carboxylate[i]
1570–1540	νN–H and νC–N in plane	Amide II[i,l,o]
1515	νC=C	Aromatics[i,o]
1465	νC–H	Aliphatics[d], organo-clay complexes[s]
1445–1350	νC–H	Methyls[d,n]
1430 (1300–1500)	νCO_3^{2-}	Carbonates[d,f,r]
1393	νCOO^-	Carboxylate[n] (*associated with BC in soil*)
1320–1230	νC–N	Amide III[i,o]
1295–1220	νC–OH, C–H in plane	Phenols, aromatics[d,i,n,q]
1170–1060	νC–O	Polysaccharides[i], nucleic acids, proteins[i,m]
1100–1000	νSi–O	Silicates (quartz)[e,f,j,o]
1050	δC–O	Carbohydrates[d,i,n]
1030–950	νSi–O	Clay minerals[o,s]
975–675	δC–H out of plane	Aromatics[l,p,q,t]
915	δAl–OH	Kaolinite and smectite[a,b,d]
875	C–O out of plane	Carbonates[o]
850–750	NH_2 out of plane	Primary amine[o]
800	Si–O	Quartz[e]
750–700	N–H wag	Secondary amine[o]
700	Si–O	Quartz[e]
700–600		Iron oxides[f]

[a]Madejova and Komadel, 2001; [b]Nayak and Singh, 2007; [c]Nguyen et al., 1991; [d]Viscarra Rossel and Behrens, 2010; [e]Churchman et al., 2010; [f]Soriano-Disla et al., 2013; [g]Ellerbrock and Gerke, 2004; [h]Haberhauer and Gerzabek, 1999; [i]Calderón et al., 2013; [j]Pedersen et al., 2011; [k]Bernier et al., 2013; [l]Leifeld, 2006; [m]Movasaghi et al., 2008; [n]Janik et al., 2007; [o]Smidt and Meissl, 2007; [p]Niemeyer et al., 1992; [q]D'Acqui et al., 1999; [r]Du and Zhou, 2011; [s]Madejová, 2003; [t]Coates, 2000.

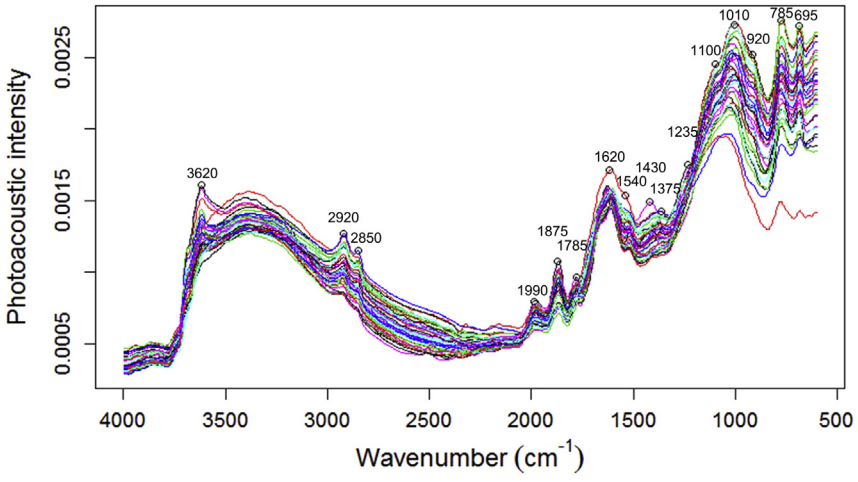

Fig. 1. FTIR-PAS spectra for the whole soil sample set ($n = 36$).

vibration of minerals from carbonates, quartz and iron oxides, but also contains aromatic C–H and amine N–H vibrations. References for these spectral interpretations can be found in Table 2.

3.3. PCA analysis

Principal component analysis was performed in order to identify the spectral regions explaining the major differences between soil spectra. The first principal component (PC1) explained most of the variance between spectra (80.5%, Fig. 2a). The loadings of PC1 indicated that this component was positively correlated with the band at 3650 cm^{-1} attributed to ν_{O-H} in clay minerals, with the band at 1020–950 cm^{-1} attributed to ν_{Si-O} from quartz and clay minerals, with the band at 950–600 cm^{-1} dominated by the vibration of δ_{Al-OH} in clay minerals at 915 cm^{-1}, carbonates at 875 cm^{-1}, iron oxides at 700–600 cm^{-1} together with aromatic and amine vibrations, probably of minor intensity in this region compared to the mineral components (Fig. 3a, Table 2). The PC1 was negatively correlated with bands assigned to organic compounds: the aliphatics band at 3000–2800 cm^{-1}, the bands centred at 1715, 1545 and 1360 cm^{-1} corresponding to carboxylic acids, carboxylate and amide II and aliphatics respectively. The second principal component (PC2) explained 9.7% of the total variance. The loadings of PC2 indicated that this component was positively correlated with the band at 3630 cm^{-1} attributed to ν_{O-H} in the clay together with the broad ν_{O-H} band at 3600–3000 cm^{-1} related to water, alcohols and phenols, with the band at 1635 cm^{-1} assigned to clay-bound water and aromatics, with band at 1425 cm^{-1} assigned to carbonates and methyls and with the carbonate band at 872 cm^{-1} (Fig. 3b). PC2 was negatively correlated with the region 3000–2500 cm^{-1} containing aliphatics C–H vibration, with the quartz overtone peaks at 1985, 1870 and 1770 cm^{-1}, the aromatic band at 1236 cm^{-1}, and the band at 1036 cm^{-1} that could be assigned to quartz and carbohydrates. The negative correlation of PC2 with the band related to quartz is consistent with the low sand content of the Ler_CL3, Ler_CL4 and Ler_CL5 samples having the highest score values on PC2 (Table 1, Fig 2a). From the analysis of the PCA loadings, it appeared that clay mineral content had a major influence on

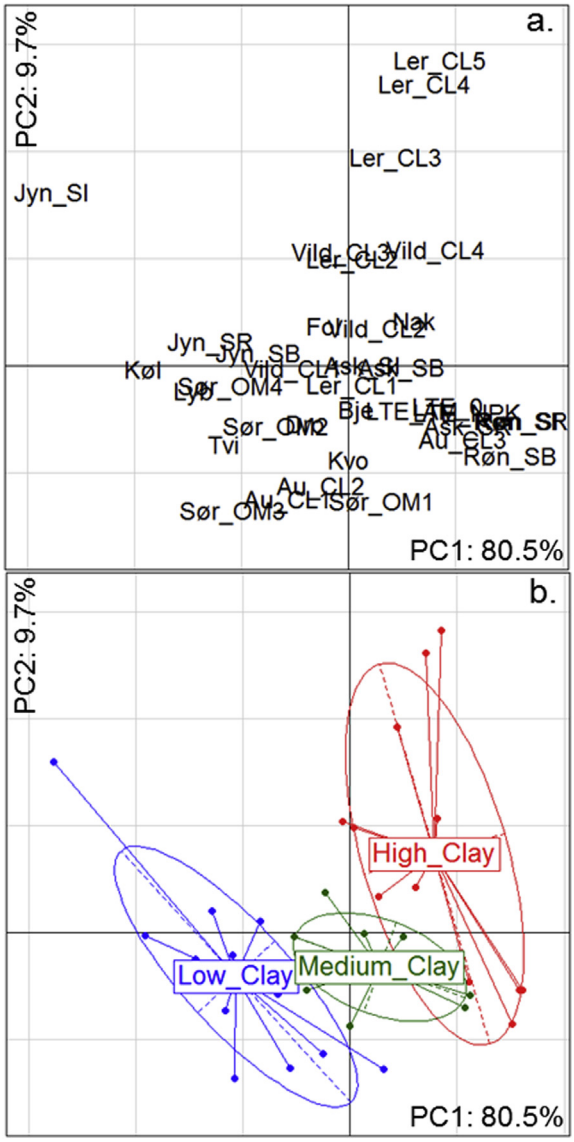

Fig. 2. Scores plot of principal component analysis based on FTIR-PAS spectra: a) partitioning the 36 soil samples within the plane defined by the two first principal components (PCs); b) clustering the data into three levels of clay content: low clay (36–62 g kg^{-1}), medium clay (73–124 g kg^{-1}) and high clay (126–402 g kg^{-1}).

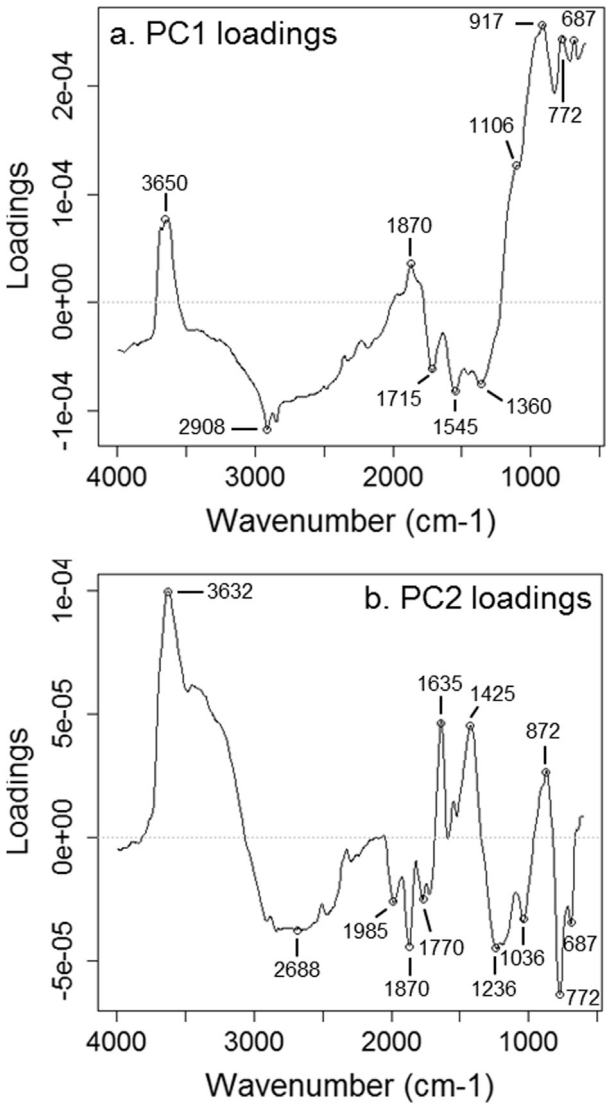

Fig. 3. Loadings of the principal component analysis based on FTIR-PAS spectra (see Fig. 2): a) loadings of the first principal component (PC1) explaining 80.5% of spectral variance; b) loadings of the second principal component explaining 9.7% of the spectral variance.

the principal spectral features of these soils. This was clearly visible when grouping the soils between three levels of clay content on the PCA plane: low clay, medium clay and high clay with ranges of clay content being 36–62 g kg^{-1}, 73–124 g kg^{-1} and 126–402 g kg^{-1} respectively (Fig. 2b). The different groups of clay were separated on PC1, with low-clay soil located on the left side of the PCA plane, whereas the medium-clay soil was located around the centre of the plane and the high-clay soil on the right side of the plane. The PC2 seemed to differentiate soils from the high-clay group, especially soils from the Lerbjerg experiment with a clay gradient (Ler_CL1–5) for which the samples with increasing clay content orientated towards the top of the PCA plane. This may reflect an increasing concentration of clay minerals (band at 3630 cm^{-1}) principally illite, smectite and vermiculite as measured in these soils in Schjønning et al. (1999). It could also reflect a decreasing concentration of sand, and possibly a higher carbonate content in these soils. This strong influence of mineral matter on the spectra renders the direct identification and interpretation of spectral bands related to organics difficult. Unravelling these therefore necessitates the use of chemometric statistical methods.

3.4. FTIR-PAS prediction of C, N and clay content

PLS regressions were computed using all soils except the soil from the Dronninglund site for TOC and total N content showing outlying TOC and total N values (see section 2.4). The Jyn_SI soil was also removed for all PLS regression analyses due to its differing spectral feature as shown by PCA analysis, which could excessively influence the calculation of PLS regression models (Fig. 2a). PLS regression produced a fair prediction model for C content, with R^2CV = 0.72 and RPD = 1.9 (Fig. 4a). Organic C content was positively correlated with the bands at 2925–2850 cm^{-1}, corresponding to ν_{C-H} from aliphatics, with the band at 1760–1630 cm^{-1} centred at 1720 cm^{-1} corresponding to $\nu_{C=O}$ from carboxylic acids and amides, with the band at 1630–1515 cm^{-1} centred at 1570 cm^{-1} attributed to ν_{N-H} from amide II together with $\nu_{C=C}$ of aromatics, carboxylates and δ_{N-H} of amine, with the band at 915 cm^{-1} corresponding to aromatics overlapping with δ_{Al-OH} from kaolinite and smectite and to a lower intensity with bands at 805 and 695 cm^{-1} that could be attributed to NH_2 out of plane from primary amines and N–H wag of secondary amines. Soil C content

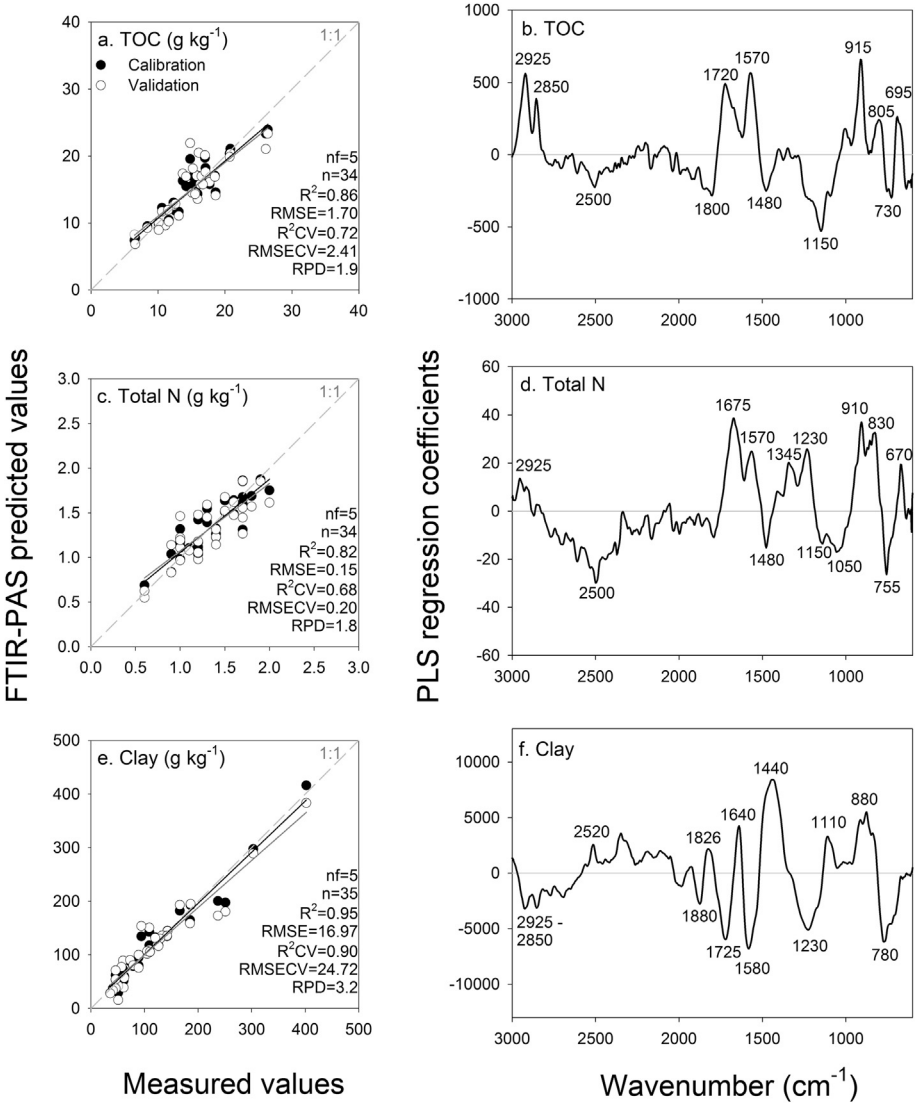

Fig. 4. Measured values *vs.* FTIR-PAS-predicted values for the calibration set (black dots, black regression line) and for cross-validated predictions (white dots, grey regression line) for total organic carbon content (TOC, a.); total nitrogen content (c.) and clay content (e.) expressed as g kg^{-1} of soil dry weight. nf denotes the number of PLS factors and *n* the number of samples. Regression coefficients of the PLS regression for total organic carbon content (b), total nitrogen content (d) and clay content (f).

was negatively correlated with the bands at 2500 cm^{-1} attributed to carbonates, with the quartz band at 1800 cm^{-1}, with the broad band spanning 1260–1060 cm^{-1} with a maximum at 1150 cm^{-1} that probably corresponds to ν_{Si-O} from quartz overlapping with ν_{C-O} from polysaccharides, nucleic acids and proteins. It was also negatively correlated with the band at 730 cm^{-1}, which could be ascribed to quartz vibrations (Fig. 4b, Table 2).

A slightly lower fraction of the variance in total N content was predicted compared with TOC, with $R^2CV = 0.68$ and RPD = 1.8 (Fig. 4c). Total N content was positively correlated with the band at 1760–1610 cm^{-1} centred at 1675 cm^{-1} corresponding to $\nu_{C=O}$ from amides and carboxylic acids, with the band at 1570 cm^{-1} attributed to ν_{N-H} and ν_{C-N} from Amide II, with the band spanning 1430–1190 cm^{-1} including the vibration of ν_{C-N} from amide III together with aromatics and phenols, with the band at 960–800 cm^{-1} attributable to aromatic rings, primary amines and δ_{Al-OH} from clay minerals with the band centred at 670 cm^{-1} that could correspond to N–H wag from secondary amine even though it has been reported at slightly higher wavenumber in the literature (750–700 cm^{-1}), or to iron oxides reported at 700–600 cm^{-1} in literature. Total N was also slightly positively correlated with the aliphatic band at 2925–2850 cm^{-1}. It was negatively correlated with the band at 2500 cm^{-1} ascribed to carbonates, with the band at 1480 cm^{-1} attributed to carbonates, aliphatics and possibly organo-clay complexes, with the bands at 1150 and 1050 cm^{-1} probably chiefly corresponding to ν_{Si-O} from clay minerals, with the band spanning 800–700 cm^{-1} centred at 755 cm^{-1} that could be attributed to ν_{Si-O} from quartz (Fig. 4d, Table 2).

As was to be expected from the PCA analysis results, a relatively large fraction of the variance in the soil clay content was predicted, with $R^2 = 0.90$ and RPD = 3.2 (Fig. 4e). The regression coefficients of the PLS regression model revealed that clay content was positively correlated chiefly with the bands at 1520–1370 cm^{-1} with a maximum at 1440 cm^{-1} ascribed to carbonates and ν_{C-H} in organo-clay complexes, with the band at 1640 cm^{-1} corresponding to ν_{H-O-H} from clay-bound water, with the band at 1230 cm^{-1} assigned to aromatics and with the band at 950–820 cm^{-1} containing the vibration of δ_{Al-OH} from kaolinite and smectite, together with δ_{C-H} and δ_{C-O} out of plane from aromatics and carbonates. It was also slightly positively correlated with the band at 2520 cm^{-1} assigned to carbonates and with the band at 1826 cm^{-1} possibly corresponding to fine quartz minerals (Fig. 4f, Table 2). The soil clay content was negatively correlated chiefly with the band at 1725 cm^{-1} assigned to carboxylic acids, with the band at 1580 cm^{-1} assigned to $\nu_{C=C}$ from aromatics and ν_{COO-}, with the band at 1320–1150 cm^{-1} centred at 1230 cm^{-1} ascribed to ν_{C-N} from amides, C–H in plane from aromatics and ν_{C-OH} from phenols, with the band at 805–675 cm^{-1} corresponding to amines, and quartz vibration. It was also slightly negatively correlated with the ν_{C-H} aliphatics band at 2925–2850 cm^{-1} and with the band at 1880 cm^{-1} ascribed to quartz overtone.

3.5. FTIR-PAS prediction of the labile fraction of SOC

PLS regression for the labile fraction of SOC (proxied by the CO_2–C evolved after 238 days of incubation: C_{238d}) yielded fair prediction models, with $R^2CV = 0.61$, RPD = 1.6 and RMSECV = 1.50% (Fig. 5a). The study of the PLS regression coefficients for C_{238d} prediction revealed that the fraction of labile C was chiefly positively correlated with the absorbance at 1520–1400 cm^{-1} that could be ascribed to aliphatics and methyls ν_{C-H} or to carbonates. It was also slightly positively correlated with the carbonate band at 2520 cm^{-1}, with the band at 1245 cm^{-1} attributed to amide III (ν_{C-N}), with the polysaccharides band at 1110 cm^{-1} and to the band at 875 cm^{-1} attributed to carbonates (Fig. 5b, Table 2). The labile fraction of SOC was chiefly negatively correlated with the band at 1620–1520 cm^{-1} centred at 1580 cm^{-1} attributed to $\nu_{C=C}$ from aromatics, carboxylates and ν_{N-H} and ν_{C-N} from amide II and δ_{N-H} from amines. It was also negatively correlated with the aliphatics band at 2925–2850 cm^{-1}, with the carboxylic acids band at 1720 cm^{-1} and with the band at 795 cm^{-1} probably corresponding to δ_{C-H} out of plane from aromatic rings.

3.6. Comparison of FTIR-PAS and NIR predictions

The performance of PLS models based on FTIR-PAS spectra was compared with the performance of PLS models based on NIR spectra and combined FTIR-PAS–NIR spectra. The results showed that FTIR-PAS-based PLS models yielded a slightly better performance for TOC, total N and labile fraction of SOC (C_{238d}) compared with NIR-based models (higher RPD and R^2CV, lower RMSECV, Table 3). Conversely, clay content was better predicted with NIR than with FTIR-PAS, with RPD = 3.8 and 3.2 respectively (Table 3). Combining FTIR-PAS and NIR spectra only improved the prediction performance for TOC, with RPD = 2.1, $R^2CV = 0.77$ compared to RPD = 1.9 and $R^2CV = 0.72$ for FTIR-PAS-based model. It is possible that the combination of FTIR-PAS and NIR spectra for the PLS model calibration could be addressed more effectively by applying more advanced data fusion techniques, such as outer product analysis (OPA), reducing the number of variables by combining FTIR-PAS and NIR spectra into a single infrared fingerprint (Barros et al.,

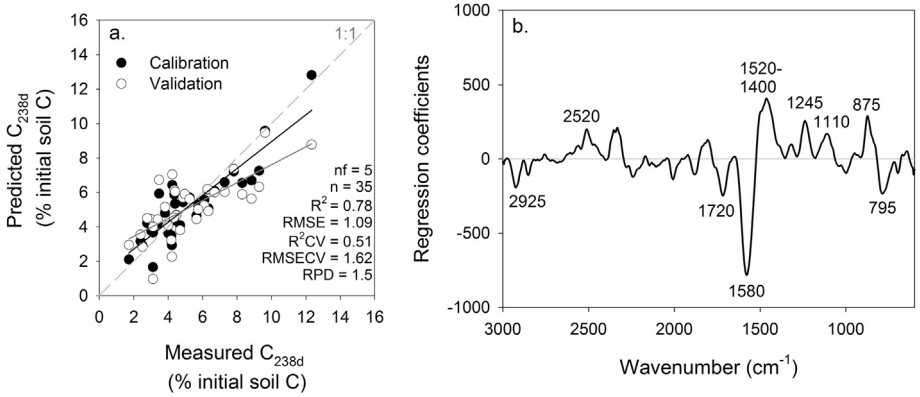

Fig. 5. Measured values *vs.* FTIR-PAS-predicted values for the calibration set (black dots, black regression line) and for cross-validated predictions (white dots, grey regression line) for the fraction of TOC evolved as CO_2 after 238 days of laboratory incubation, taken as an indicator of the labile fraction of soil organic C (C_{238d}) (a). nf denotes the number of PLS factors and *n* the number of samples. Regression coefficients of the PLS regression models based on FTIR-PAS spectra for C_{238d} (b).

Table 3
Performance of PLS regression prediction models based on FTIR-PAS spectra, NIR spectra and combined FTIR-PAS + NIR spectra. nf denotes the number of factors in the PLS model and *n* the number of samples. Performance calculations are based on cross-validation results.

Y variables	*X* variables	*n*	nf	R^2CV	RMSECV	RPD
TOC (g kg^{-1})	FTIR-PAS	34	5	0.72	2.41	1.9
	NIR	34	3	0.62	2.79	1.6
	FTIR-PAS + NIR	34	8	0.77	2.16	2.1
Total N content (g kg^{-1})	FTIR-PAS	34	5	0.68	0.20	1.8
	NIR	34	9	0.65	0.21	1.7
	FTIR-PAS + NIR	34	7	0.66	0.21	1.7
Clay (g kg^{-1})	FTIR-PAS	35	5	0.90	24.7	3.2
	NIR	35	9	0.93	21.2	3.8
	FTIR-PAS + NIR	35	5	0.93	21.8	3.7
C_{238d} (% initial TOC)	FTIR-PAS	35	6	0.61	1.50	1.6
	NIR	35	3	0.53	1.61	1.5
	FTIR-PAS + NIR	35	7	0.60	1.55	1.5

1997; Cecillon et al., 2012). However, an approach of this kind was not attempted here.

4. Discussion

4.1. Validity of FTIR-PAS combined with PLS regression for predicting soil properties and deriving information on soil chemical composition

Principal component analysis revealed that the variance between FTIR-PAS spectra was mostly explained by soil mineral matrix (Fig. 2). It is therefore necessary to use chemometric methods as PLS regression to identify regions related to specific organic components from FTIR-PAS spectra. The PLS regression models produced in this study for TOC and total N showed lower accuracy compared to the values reported by Soriano-Disla et al. (2013) in a review of using MIR and NIR spectroscopy for predicting soil properties. This could be due to the narrow range of values in the present dataset, limiting the possibility of obtaining large R^2 values. However, applying a similar statistical procedure, FTIR-PAS performed slightly better than NIR for predicting TOC, total N and C_{238d}. Better prediction results could be obtained by applying jackknife techniques or other variable selection methods for removing non-significant wavelengths in PLS models (e.g. Martens and Martens, 2000). However this is risky without proper verification of model robustness using an independent validation set of samples. Unfortunately, this could not be achieved in this study due to the relatively few soil samples in our dataset, which only allowed us to use cross-validation. It is important to highlight that producing models for operational predictions is beyond the scope of this study, which was merely to assess the potential of FTIR-PAS for building prediction models and interpretation of the regression coefficients of the PLS models. Studying these coefficients made it possible to assess the relationships between predicted soil constituents and functional groups and molecules contributing to the prediction, which is a prerequisite for producing robust and transferable prediction models. TOC was chiefly positively correlated with the spectral bands ascribed to aliphatics, carboxylic acids, amides and aromatics, which represent the major carbon forms in soil (von Lützow et al., 2006). Total N was also positively correlated with the major soil nitrogenous compounds: amides and amines. Clay content was mostly correlated with spectral bands related to clay minerals, clay bound water or organo-clay complexes. Overall, the analysis of the PLS regression coefficient for TOC, total N and clay content showed the consistency between the chemical bonds/compounds used for prediction and the constituents to be predicted. It confirms that FTIR-PAS can be used to interpret the chemical composition of organic and mineral fractions of soil. Another advantage of FTIR-PAS is makes it possible to finely characterize the surface of soil particles and allows depth profiling analysis. These features could be used in a future study to specifically characterize the organic molecules on surface coatings of soil particles as opposed to those incorporated into microaggregates (McClelland et al., 2006; Churchman et al., 2010; Du and Zhou, 2011).

4.2. Use of FTIR-PAS to characterize the chemical composition of the labile fraction of SOC

The labile fraction of SOC, here proxied by the CO_2–C evolved after 238 days of incubation (C_{238d}) was chiefly positively correlated with the band at 1520–1400 cm^{-1}, which could be ascribed to aliphatic and methyl compounds (Fig. 5b, Table 2). Aliphatics and methyls of plant origin are considered as intrinsically easily degradable (Smidt and Meissl, 2007; Marschner et al., 2008), but aliphatics are non-specific compounds that also originate from microbially-processed OM which might be stabilised in soil (Grandy and Neff, 2008). The later might explain the negative correlation found between the labile fraction of SOC and the aliphatic band at 3000–2800 cm^{-1}, which could correspond to microbially-derived aliphatic compounds. Aliphatics vibrations in the region of 3000–2800 cm^{-1} have also been shown to be an important constituent of the clay sized fraction of SOC, which typically has a slow turnover time (Balesdent, 1996; Leifeld, 2006). This is supported by the review of Amelung et al. (2008), showing that aliphatics have a highly variable residence time in soil. The bands at 1520–1400 cm^{-1} could also be ascribed to carbonates, which is supported by the positive correlation of C_{238d} with the bands at 2520 and 875 cm^{-1}, also ascribed to carbonates. Most of the soils had a pH ranging from neutral to slightly acidic, and are therefore not likely to contain carbonates. Only the Ler_CL4 soil (pH = 7.5) and the Ler_CL5 soil (pH = 7.6) from the Lerbjerg site had pH of 7.5 and 7.6 are likely to contain carbonates (Table 1). These two soils also had the highest C_{238d} values (9.62 and 12.33% of initial TOC, respectively, Table 1). It is therefore likely that the positive correlation found between C_{238d} and spectral bands assigned to carbonates originate from covariance due to the influence of these two soils on the PLS model calculation rather than from an actual chemical relationship between labile SOC and carbonates. The labile fraction of SOC was also slightly positively correlated with spectral bands related to amides and polysaccharides. The latter are considered as intrinsically labile even though they can also be found in stabilized SOC (Amelung et al., 2008).

The most important correlation between the labile fraction of SOC and FTIR-PAS spectra was the negative correlation with the band at 1620–1520 cm^{-1}. This band is attributed to aromatics, carboxylates, amide II (ν_{N-H} and ν_{C-N} in plane) and amines. The labile fraction of SOC was also negatively correlated with the band at 1720 cm^{-1} ascribed to carboxylic acids and with the band at 795 cm^{-1} attributed to aromatics. In a previous study, Janik et al. (2007) found the band at 1597–1570 cm^{-1} to be correlated with char-C, confirming the highly aromatic nature of C vibrating in this region. The negative correlation of the labile fraction of SOC with carboxylic acids, carboxylate and aromatic groups could be explained by these compounds being protected against biodegradation due to the recalcitrant nature of aromatic structures, due to organo-mineral associations, since these groups are reactive for interaction with mineral surfaces, most probably through polyvalent cation bridges with clay surfaces, or due to the hydrophobic surfaces of aromatic and carboxylic-C, reducing surface wettability and thus reducing the accessibility of OM to microorganisms and

their enzymes (von Lützow et al., 2006). The negative correlation of labile SOC with amines and amides confirms the abundance of nitrogenous compounds in stabilized SOC reported by several studies (Rillig et al., 2007; Amelung et al., 2008; Knicker, 2011). Nitrogenous compounds such as amino sugar are probably of microbial origin in soil, as plants do not contain significant amount of amino sugars (Amelung et al., 2008).

5. Conclusions

FTIR-PAS spectroscopy offers the advantage over reflectance spectroscopy that sample opacity has little effect on the PAS signal, that makes it particularly attractive for soil characterisation. FTIR-PAS performed similar to or better than near infrared spectroscopy for the prediction of total organic carbon, total N content and the fraction of labile soil organic carbon, while the prediction of clay content was better using NIR spectroscopy. FTIR-PAS spectroscopy offers the advantage over NIR that it is possible to identify and interpret the functional groups and molecules that are positively or negatively correlated with the constituent for prediction purposes by interpreting the regression coefficients of the PLS regression models. These coefficients revealed a close agreement between the predicted constituents and the chemical species contributing to the prediction for total organic C, total N and clay content. This kind of verification of the agreement between the spectral regions used in prediction models and the soil organic matter chemistry is crucial if over-calibration of the models is to be avoided and regression models are to be transferred to other sets of samples. The identification and interpretation of the spectral bands that correlated positively and negatively with the labile fraction of soil organic carbon revealed that bands corresponding to aliphatic, methyls, amide III (ν_{C-N}) and polysaccharides were positively correlated with the labile fraction of SOC, whereas bands corresponding to aromatics, amides II, amines and carboxylic acids were negatively correlated with this fraction. An interpretation of this kind therefore provided an advance in understanding of the chemical composition of labile C in soil, which is a fraction that is difficult to separate experimentally.

Overall, this study provided proof of the concept that FTIR-PAS spectroscopy can be added to the set of spectroscopic tools used to predict soil properties both quickly and inexpensively, including SOM lability or stability after the proper calibration of regression models, and used to characterise soil organic matter.

Acknowledgements

The research leading to these results has received funding from the People Programme (Marie Curie Actions, Intra-European Fellowship) of the European Union's Seventh Framework Programme FP7/2007–2013/under REA grant agreement n° 298561.

References

Amelung, W., Brodowski, S., Sandhage-Hofmann, A., Bol, R., 2008. Chapter 6 combining biomarker with stable isotope analyses for assessing the transformation and turnover of soil organic matter. In: Donald, L.S. (Ed.), Advances in Agronomy. Academic Press, pp. 155–250.

Balesdent, J., 1996. The significance of organic separates to carbon dynamics and its modelling in some cultivated soils. Eur. J. Soil Sci. 47 (4), 485–493.

Barros, A.S., Safar, M., Devaux, M.F., Robert, P., Bertrand, D., Rutledge, D.N., 1997. Relations between mid-infrared and near-infrared spectra detected by analysis of variance of an intervariable data matrix. Appl. Spectrosc. 51 (9), 1384–1393.

Bernier, M.-H., Levy, G.J., Fine, P., Borisover, M., 2013. Organic matter composition in soils irrigated with treated wastewater: FT-IR spectroscopic analysis of bulk soil samples. Geoderma 209–210 (0), 233–240.

Bruun, S., Stenberg, B., Breland, T.A., Gudmundsson, J., Henriksen, T.M., Jensen, L.S., Korsaeth, A., Luxhoi, J., Palmason, F., Pedersen, A., Salo, T., 2005. Empirical predictions of plant material C and N mineralization patterns from near infrared spectroscopy, stepwise chemical digestion and C/N ratios. Soil Biol. Biochem. 37 (12), 2283–2296.

Calderón, F., Haddix, M., Conant, R., Magrini-Bair, K., Paul, E., 2013. Diffuse-reflectance Fourier-transform mid-infrared spectroscopy as a method of characterizing changes in soil organic matter. Soil Sci. Soc. Am. J. 77 (5), 1591–1600.

Capriel, P., Beck, T., Borchert, H., Gronholz, J., Zachmann, G., 1995. Hydrophobicity of the organic matter in arable soils. Soil Biol. Biochem. 27, 1453–1458.

Cecillon, L., Certini, G., Lange, H., Forte, C., Strand, L.T., 2012. Spectral fingerprinting of soil organic matter composition. Org. Geochem. 46, 127–136.

Chang, C., Laird, D.A., Mausbach, M.J., Hurburgh Jr., C.R., 2001. Near-infrared reflectance spectroscopy-principal components regression analyses of soil properties. Soil Sci. Soc. Am. J. 65 (2), 480–490.

Chessel, D., Dufour, A.B., Thioulouse, J., 2004. The ade4 package – I: one-table methods. R News, 5–10.

Churchman, G.J., Foster, R.C., D'Acqui, L.P., Janik, L.J., Skjemstad, J.O., Merry, R.H., Weissmann, D.A., 2010. Effect of land-use history on the potential for carbon sequestration in an Alfisol. Soil Tillage Res. 109, 23–35.

Coates, J., 2000. Interpretation of infrared spectra, a practical approach. In: Meyers, R.A. (Ed.), Encyclopedia of Analytical Chemistry. John Wiley & Sons, pp. 10815–10837.

D'Acqui, L.P., Churchman, G.J., Janik, L.J., Ristori, G.G., Weissmann, D.A., 1999. Effect of organic matter removal by low-temperature ashing on dispersion of undisturbed aggregates from a tropical crusting soil. Geoderma 93, 311–324.

Du, C., He, Z., Zhou, J., 2013. Characterization of soil humic substances using mid-infrared photoacoustic spectroscopy. In: Xu, J., Wu, J., He, Y. (Eds.), Functions of Natural Organic Matter in Changing Environment. Springer, Netherlands, pp. 43–47.

Du, C.W., Zhou, J.M., 2011. Application of infrared photoacoustic spectroscopy in soil analysis. Appl. Spectrosc. Rev. 46 (5), 405–422.

Ellerbrock, R.H., Gerke, H.H., 2004. Characterizing organic matter of soil aggregate coatings and biopores by Fourier transform infrared spectroscopy. Eur. J. Soil. Sci. 55 (2), 219–228.

Gerzabek, M.H., Antil, R.S., Kogel-Knabner, I., Knicker, H., Kirchmann, H., Haberhauer, G., 2006. How are soil use and management reflected by soil organic matter characteristics: a spectroscopic approach. Eur. J. Soil Sci. 57 (4), 485–494.

Grandy, A.S., Neff, J.C., 2008. Molecular C dynamics downstream: the biochemical decomposition sequence and its impact on soil organic matter structure and function. Sci. Total Environ. 404 (2–3), 297–307.

Haberhauer, G., Gerzabek, M.H., 1999. Drift and transmission FT-IR spectroscopy of forest soils: an approach to determine decomposition processes of forest litter. Vib. Spectrosc. 19 (2), 413–417.

Janik, L.J., Skjemstad, J.O., Shepherd, K.D., Spouncer, L.R., 2007. The prediction of soil carbon fractions using mid-infrared-partial least square analysis. Aust. J. Soil Res. 45 (2), 73–81.

Knicker, H., 2011. Soil organic N – an under-rated player for C sequestration in soils? Soil Biol. Biochem. 43, 1118–1129.

Leifeld, J., 2006. Application of diffuse reflectance FT-IR spectroscopy and partial least-squares regression to predict NMR properties of soil organic matter. Eur. J. Soil Sci. 57 (6), 846–857.

Madejova, J., Komadel, P., 2001. Baseline studies of the clay minerals society source clays: infrared methods. Clay Clay Min. 49 (5), 410–432.

Madejová, J., 2003. FTIR techniques in clay mineral studies. Vib. Spectrosc. 31, 1–10.

Marschner, B., Brodowski, S., Dreves, A., Gleixner, G., Gude, A., Grootes, P.M., Hamer, U., Heim, A., Jandl, G., Ji, R., Kaiser, K., Kalbitz, K., Kramer, C., Leinweber, P., Rethemeyer, J., Schaffer, A., Schmidt, M.W.I., Schwark, L., Wiesenberg, G.L.B., 2008. How relevant is recalcitrance for the stabilization of organic matter in soils? J. Plant Nutr. Soil Sci. 171 (1), 91–110.

Martens, H., Martens, M., 2000. Modified Jack-knife estimation of parameter uncertainty in bilinear modelling by partial least squares regression (PLSR). Food Qual. Prefer. 11 (1–2), 5–16.

McClelland, J.F., Jones, R.W., Bajic, S.J., 2006. Photoacoustic Spectroscopy, Handbook of Vibrational Spectroscopy. John Wiley & Sons, Ltd.

Movasaghi, Z., Rehman, S., Rehman, I.U., 2008. Fourier transform infrared (FTIR) spectroscopy of biological tissues. Appl. Spectrosc. Rev. 43 (2), 134–179.

Nayak, P., Singh, B.K., 2007. Instrumental characterization of clay by XRF, XRD and FTIR. Bull. Mater. Sci. 30 (3), 235–238.

Nguyen, T.T., Janik, L.J., Raupach, M., 1991. Diffuse reflectance infrared Fourier-transform (drift) spectroscopy in soil studies. Aust. J. Soil Res. 29 (1), 49–67.

Niemeyer, J., Chen, Y., Bollag, J.M., 1992. Characterization of humic acids, composts, and peat by diffuse reflectance Fourier-transform infrared-spectroscopy. Soil Sci. Soc. Am. J. 56 (1), 135–140.

Paul, E.A., Morris, S.J., Conant, R.T., Plante, A.F., 2006. Does the acid hydrolysis-incubation method measure meaningful soil organic carbon pools? Soil Sci. Soc. Am. J. 70 (3), 1023–1035.

Pedersen, J.A., Simpson, M.A., Bockheim, J.G., Kumar, K., 2011. Characterization of soil organic carbon in drained thaw-lake basins of Arctic Alaska using NMR and FTIR photoacoustic spectroscopy. Org. Geochem. 42 (8), 947–954.

Peltre, C., Thuriès, L., Barthès, B., Brunet, D., Morvan, T., Nicolardot, B., Parnaudeau, V., Houot, S., 2011. Near infrared reflectance spectroscopy: a tool to characterize the composition of different types of exogenous organic matter and their behaviour in soil. Soil Biol. Biochem. 43 (1), 197–205.

R Development Core Team, 2012. R: a Language and Environment for Statistical Computing, Version 2.15.2. R Foundation for Statistical Computing, Vienna, Austria.

Rillig, M., Caldwell, B., Wösten, H., Sollins, P., 2007. Role of proteins in soil carbon and nitrogen storage: controls on persistence. Biogeochemistry 85 (1), 25–44.

Schjønning, P., Thomsen, I.K., Møberg, J.P., de Jonge, H., Kristensen, K., Christensen, B.T., 1999. Turnover of organic matter in differently textured soils: I. Physical characteristics of structurally disturbed and intact soils. Geoderma 89 (3–4), 177–198.

Schmidt, M.W.I., Torn, M.S., Abiven, S., Dittmar, T., Guggenberger, G., Janssens, I.A., Kleber, M., Kogel-Knabner, I., Lehmann, J., Manning, D.A.C., Nannipieri, P., Rasse, D.P., Weiner, S., Trumbore, S.E., 2011. Persistence of soil organic matter as an ecosystem property. Nature 478 (7367), 49–56.

Smidt, E., Meissl, K., 2007. The applicability of Fourier transform infrared (FT-IR) spectroscopy in waste management. Waste Manag. 27 (2), 268–276.

Soriano-Disla, J.M., Janik, L.J., Viscarra Rossel, R.A., MacDonald, L.M., McLaughlin, M.J., 2013. The performance of visible, near-, and mid-infrared reflectance spectroscopy for prediction of soil physical, chemical, and biological properties. Appl. Spectrosc. Rev. 49 (2), 139–186.

Stevenson, F.J., 1994. Humus Chemistry: Genesis, Composition, Reactions. Wiley & Sons, New York, p. 496.

Stumpe, B., Weihermuller, L., Marschner, B., 2011. Sample preparation and selection for qualitative and quantitative analyses of soil organic carbon with mid-infrared reflectance spectroscopy. Eur. J. Soil Sci. 62 (6), 849–862.

Thomsen, I.K., Bruun, S., Jensen, L.S., Christensen, B.T., 2009. Assessing soil carbon lability by near infrared spectroscopy and NaOCl oxidation. Soil Biol. Biochem. 41 (10), 2170–2177.

Viscarra Rossel, R.A., Behrens, T., 2010. Using data mining to model and interpret soil diffuse reflectance spectra. Geoderma 158 (1–2), 46–54.

Viscarra Rossel, R.A., Walvoort, D.J.J., McBratney, A.B., Janik, L.J., Skjemstad, J.O., 2006. Visible, near infrared, mid infrared or combined diffuse reflectance spectroscopy for simultaneous assessment of various soil properties. Geoderma 131 (1–2), 59–75.

van Groenigen, J.W., Mutters, C.S., Horwath, W.R., van Kessel, C., 2003. NIR and DRIFT-MIR spectrometry of soils for predicting soil and crop parameters in a flooded field. Plant Soil 250, 155–165.

von Lützow, M., Kögel-Knabner, I., Ekschmitt, K., Matzner, E., Guggenberger, G., Marschner, B., Flessa, H., 2006. Stabilization of organic matter in temperate soils: mechanisms and their relevance under different soil conditions – a review. Eur. J. Soil. Sci. 57 (4), 426–445.

Wetzel, D.L., 1983. Near-infrared reflectance analysis. Anal. Chem. 55 (12), 1165A–1176A.

View publication stats